

The Lowest Singlet (n,π^*) and (π,π^*) Excited States of the Hydrogen-Bonded Complex between Water and Pyrazine

Zheng-Li Cai and Jeffrey R. Reimers*

School of Chemistry, The University of Sydney, NSW 2006, Australia

Received: September 7, 2006; In Final Form: November 27, 2006

The hydrogen bonding between water and pyrazine in its ground, lowest (n,π^*), and lowest (π,π^*) states is investigated using density-functional theory (DFT), time-dependent density function theory (TD-DFT), coupled-cluster singles and doubles (CCSD) theory and equation-of-motion coupled cluster (EOM-CCSD) theory. For all states, the minimum-energy configuration is found to be an orthodox linear hydrogen-bonded species, with the bond strength increasing by 0.4 kcal mol⁻¹ upon formation of the (π,π^*) state and decreasing by 1.0 kcal mol⁻¹ upon formation of the (n,π^*) state. The calculated solvent shifts for the complexes match experimental data and provide a basis for the understanding of the aqueous solvation of pyrazine, and the excited-state complexes are predicted to be only short-lived, explaining the failure of molecular beam experiments to observe them. Quite a different scenario for hydrogen bonding to the (n,π^*) excited state is found compared to those of H₂O:pyridine and H₂O:pyrimidine: for pyridine linear hydrogen bonds are unstable and hydrogen bonds to the electron-enriched π cloud are strong, whereas for pyrimidine the excitation localizes on the nonbonded nitrogen leaving the hydrogen-bonding unaffected. For H₂O:pyrazine, the (n,π^*) excitation remains largely delocalized, providing a distinct intermediary scenario.

1. Introduction

Hydrogen bonding involving heteroaromatic rings such as those in azines and diazines is very important as it plays an important role in the structure and function of many biological systems.^{1–3} Although hydrogen bonding to molecules in their ground electronic state has been widely investigated by different spectroscopic^{4–19} and theoretical^{1,18,20–42} methods, much less is known about hydrogen bonding to molecules in excited states. Archetypal studies include the absorption and fluorescence studies that culminated in the work of Baba, Goodman, and Valenti,⁴ supersonic molecular jet spectroscopy pioneered by Bernstein et al.,^{8,9} and computations pioneered by Del Bene.^{20–22,28,43} The (n,π^*) states are particularly pertinent as the electronic transition removes one of the lone-pair electrons that directly participate in the hydrogen bonding. The properties of the (π,π^*) excited states are also relevant to proton-transfer and tautomerization in azines.^{44,45}

The basic concepts involved were elucidated in 1966 by Baba, Goodman, and Valenti⁴ who studied the absorption and fluorescence spectra of pyridine, pyridazine, pyrimidine and pyrazine in dilute solution in a variety of hydrogen-bonding and non-hydrogen-bonding solvents. They found that in hydrogen-bonding solvents the hydrogen bond formed between the solute in its ground electronic state and solvent molecules gives a large blue shift in the (n,π^*) absorption transition but only small changes in the corresponding fluorescence spectrum. Dielectric solvation theories^{27,46–48} express these solvent shifts as

$$\Delta U = \frac{2\epsilon - 2}{2\epsilon + 1} \frac{1}{a^3} \mu_i (\mu_f - \mu_i) - \frac{n^2 - 1}{2n^2 + 1} \frac{1}{a^3} |\mu_f - \mu_i|^2 \quad (1)$$

where μ_i and μ_f are the dipole moment vectors of the initial

and final states solvated outside a cavity of radius a by a material of dielectric constant ϵ and refractive index n . As the coefficient of the first term is much larger than that for the second, and as only the first term can give rise to a blue shift, Baba et al. qualitatively interpreted the experimental data as indicating a large dipole moment (ca. 3 D) on the ground state and a nearly zero dipole moment in the excited state. From this they concluded that the hydrogen bonding is broken in the (n,π^*) singlet excited state of pyridine and the diazines. Their analysis appears valid for pyridine, but for the diazines it is incomplete as it does not properly address the issue of the localization/delocalization of the (n,π^*) excitation over the two nitrogen atoms. In the ground state, liquid-structure simulations indicate two hydrogen bonds are formed to the diazines.^{24,25,29,30} In the excited state, if the excitation localizes onto one nitrogen atom, then this atom becomes analogous to the nitrogen in pyridine and the other atom is unaffected. One would thus expect that the hydrogen bond to the unaffected nitrogen would remain intact and the other hydrogen bond would break. However, if the excitation is delocalized over both diazine nitrogen atoms, then each atom will have 1.5 electrons with which it may form hydrogen bonds to its environment, and it is not clear a priori whether or not hydrogen bonds are likely to form.^{26,29,30} Before the effects of through-bond interactions were known, strong interactions between nitrogen lone pairs were not expected and thus the excitation in pyrimidine and pyrazine (at least) were believed to be localized excitations,²⁹ even for uncomplexed pyrazine.⁴⁹ For pyrazine in the gas phase, however, high-resolution spectroscopy clearly indicates that the (n,π^*) excitation is delocalized in isolated pyrazine.²⁹

Wanna, Menapace and Bernstein^{8,9} have studied the hydrogen bonded and nonbonded van der Waals clusters, diazines such as pyridazine, pyrazine, pyrimidine and benzene (solutes) and C_nH_{2n+2}, NH₃ and H₂O (solvents) by the techniques of supersonic molecular jet spectroscopy and two-color time-of-

* Corresponding author. E-mail: reimers@chem.usyd.edu.au.

flight mass spectroscopy. They did not observe pyridazine, pyrazine, or pyrimidine water clusters, however, and concluded that the excited states of these clusters must be dissociative. Stable excited states have indeed been observed for a range of other azine complexes with hydrogen-bond donors.⁶

The electronic and geometrical structure of pyridine and the diazines in their (n, π^*) excited states in clusters and in aqueous solution have been simulated by Karelson and Zerner,^{50,51} Zeng, Hush and Reimers,^{25–27,29,30,52} Gao and Byun,³² Almeida et al.,³⁶ Mennucci,³⁹ Cossi and Barone,³⁸ and very recently de Monte et al.⁴² using combinations of semiempirical INDO/S^{36,50,51} or AM1³² methods with continuum solvation models,^{50,51} QM/MM methods,^{32,53} analytical all-atom electrostatic methods,^{25,27,29,30,52} time-dependent density functional theory,^{38,39} and the continuum solvation model COSMO in combination with multireference configuration interaction with singles and doubles (MR-CISD).⁴² Qualitatively, the nature of hydrogen bonding and calculated solvent shifts are found to be very sensitive to the details of the potential-energy surfaces or electronic structure method used.

A focus of these studies has been understanding the process by which the observed dilute-solution blue shift of the (n, π^*) band arises; this shift is observed to be in the range between 1600 and 2000 cm^{-1} for pyrazine.^{4,29} Zeng et al., using an AMBER⁵⁴-based molecular-mechanics potential parametrized using multireference configuration-interaction calculations,²⁹ calculated the solvent structure and from this predicted a blue shift of $2000 \pm 500 \text{ cm}^{-1}$, in good agreement with the experimental data. Of this shift, 1200 cm^{-1} was attributed to the H_2O :pyrazine complex, in excess of the experimental value⁸ of 580 cm^{-1} , and the remainder to long-range interactions. Alternatively, using TD-DFT methods involving use of the polarizable-continuum model (PCM) to implicitly describe the effects of the solvent structure, Cossi and Barone³⁸ predicted a shift of 445–1416 cm^{-1} for dilute pyrazine in solution. Also Mennucci,³⁹ using TD-DFT methods implemented with an integral equation formalism-polarizable continuum model (IEF-PCM) for the solvent structure, predicted a shift of 400–1300 cm^{-1} , and Monte et al.⁴² using high level MR-CISD(+Q) based on the COSMO solvent model predicted 1000–1700 cm^{-1} . It is hence clear that proper understanding of this problem requires the use of both high-quality geometrical structures for the solvent and high-quality electronic-structure computations. All of the above methods rely on structures for which at least one aspect is crudely estimated, and all involve significant approximations to the evaluation of the transition energy at those geometries. Although modern computational methods such as Carr–Parinello excited-state molecular dynamics⁵⁵ and mixed quantum-mechanics molecular-mechanics simulations offer the possibility of improved liquid-state simulations, reliable calculations are not yet technically feasible.

In this work we consider not the problem of the aqueous solvation of pyrazine but rather the simpler, intricately related problem of the properties of the H_2O :pyrazine complex, applying state of the art methods to determine both its geometrical structure and the influence of this structure on its electronic absorption spectrum. Clearly, any computational problem applied to solve the full problem of interacting chromophore and solvent molecules must be first demonstrated to perform satisfactorily when applied to this dimer.

Although the hydrogen bonding in water and azines or diazine complexes in their ground electronic states has been widely investigated using high-level electronic-structure methods,^{1,11,14–17,29–31,41,56–64} only Del Bene^{20–22,28} and ourselves^{41,64} have similarly considered excited-state phenomena.

Structural studies have only been performed for the $\text{HF}:\text{H}_2\text{CO}$ complex by Del Bene et al.⁴³ and by ourselves^{41,64} for H_2O :pyridine and H_2O :pyrimidine. Each of these studies reveals new or unexpected *motifs* for hydrogen bonding: for H_2CO this is a structure with hydrogen bond formation occurring at the oxygen in the C_s symmetry plane, for H_2O :pyridine a strong hydrogen bond is found from a water hydrogen to the electron-enhanced aromatic π cloud, but for H_2O :pyrimidine the ground-state structure remains dominant. As pyrazine, like pyrimidine, has two lone pairs per molecule, and as the intramolecular interactions between them are known to be quite different, it is not clear a priori if hydrogen bonding to the excited states of pyrazine will be similar to that for either H_2O :pyridine or H_2O :pyrimidine or will display yet another motif.

Studies of azine–water clusters are of interest not only in terms of the mechanism of aqueous solvent shifts but also in their own right as these clusters can be made in molecular beam^{8,9} and matrix-isolation¹¹ experiments. A key property is whether or not the vertically excited complex is expected to predissociate. Our previous studies⁴¹ of H_2O :pyridine predict that the additional energy provided to vertically excite the complex, the absorption “blue shift”, significantly exceeds the dissociation energy of the complex in its (n, π^*) excited state. As a result, H_2O :pyridine is expected to directly dissociate following (n, π^*) excitation. Similar calculations for H_2O :pyrimidine predict that the vertically excited state should be long-lived, however, due to the localization of the (n, π^*) excitation on the nonbonded nitrogen in this complex. However, years earlier, our more primitive calculations employing ab initio-optimized AMBER force fields^{26,27,29} predicted that for all diazines the blue shift is actually less than that required for direct dissociation, suggesting that stable excited-state complexes could be obtained for all of the diazines after vertical excitation. These molecular mechanics calculations were based on the assumption that the delocalized nature of the (n, π^*) excitation for the diazines in the gas phase was retained after hydrogen-bond formation, and that the solvent acted merely to perturb this structure. However, subsequent high-level calculations for the H_2O :pyrimidine complex showed this assumption to be incorrect.⁶⁴ Hence the nature of the excited-state solvation of H_2O :pyrazine appears of significant interest.

Specifically, we determine the structures, bond energies, and vibration frequencies of H_2O :pyrazine in its ground and first (n, π^*) and (π, π^*) excited states using analogous methods for both the ground and excited states. We use density functional theory (DFT) with the B3LYP⁶⁵ and BLYP^{66,67} functionals and coupled-cluster theory (CCSD⁶⁸) to study ground states, employing the related time-dependent methods time-dependent density-functional theory (TD-DFT) and equation-of-motion coupled-cluster (EOM-CCSD⁶⁹) theory to study electronic excited states. Some test calculations are also performed using the more accurate but more expensive similarity-transformed equations of motion (STEOM) coupled-cluster⁷⁰ method. This work follows from our previous comprehensive treatise of the excited-state manifolds of isolated pyrazine^{71,72} in which we considered in detail the energetics, structures, and vibrational motions of this molecule in a variety of its excited states.

2. Computational Details

A variety of computational schemes are used as is appropriate for the optimization of geometries, accurate structural energy determination, and vibrational analyses of hydrogen-bonded dimers in their ground and excited electronic states. Direct B3LYP⁶⁵ geometry optimizations and frequency calculations

TABLE 1: Comparison of Calculated and Experimental Properties^a of the Water in Its Ground State and Pyrazine in Its ¹A_g Ground State (GS), First Singlet (n,π*) ¹B_{3u} and First Singlet (π,π*) ¹B_{2u} Excited States

methods ^b	basis	rms error in property							
		bond length/Å		bond angle/deg		frequency ^c /cm ⁻¹			
		H ₂ O	pyrazine GS	H ₂ O	pyrazine GS	H ₂ O	GS	(n,π*)	(π,π*)
(TD-)B3LYP	cc-pVDZ	0.011	0.007	1.78	0.60	42	21		
(TD-)B3LYP	aug-cc-pVDZ	0.007	0.005	0.23	0.55	23	21		
(EOM-)CCSD	cc-pVDZ	0.007	0.010	2.34	0.71	10	29	82	46
(EOM-)CCSD	aug-cc-pVDZ	0.007	0.010	0.36	0.57	24			

^a From refs 83, 85, and 86. ^b B3LYP or CCSD for the ground state, TD-B3LYP or EOM-CCSD for the excited states. ^c Using scale factors⁷⁸ of 0.9614 and 0.95 for the B3LYP or TD-B3LYP and CCSD or EOM-CCSD calculations, respectively.

were performed for the ground-state using GAUSSIAN-98.⁷³ TD-B3LYP calculations were performed by TURBOMOLE⁷⁴ using the “M3” integrating grid and the energy convergence criterion set to 10⁻¹⁰ au. CCSD⁶⁸ ground-state and EOM-CCSD⁶⁹ or STEOM⁷⁰ excited-state calculations were performed using analytical first derivatives by ACES-II.⁷⁵ Atomic Gaussian basis sets were employed in all of these calculations. In addition, TD-BLYP^{66,67} geometry optimizations were performed for the excited states of hydrogen-bonded complexes using the CPMD⁵⁵ package; in these, a single complex was placed in a large cubic unit cell of length 15 Å, and a plane-wave basis set was used truncated at an energy of 65 Rydbergs (32.5 au).

Dunning’s correlation-consistent polarized valence double- ζ basis set cc-pVDZ⁷⁶ was used for all geometry optimizations involving atomic basis sets. This is the smallest basis set that could provide a realistic description of the nature of both the excited states and the hydrogen bonds; larger basis sets will result in quantitative improvements in accuracy but are not feasible to apply for the method used herein. In addition, Dunning’s augmented aug-cc-pVDZ⁷⁷ is used for single-point calculations of binding energies evaluated at these (and other) optimized geometries; some test structural optimizations were also performed using the aug-cc-pVDZ basis. All binding energies are corrected for the zero-point energy (ZPE) based on harmonic force fields determined using the cc-pVDZ basis set. Although use of augmented basis sets is essential for quantitative vibrational analyses of significant modes such as intermolecular stretches, they are not essential for the determination of zero-point energies and hence the smaller cc-pVDZ basis is used herein for this purpose. However, the normal-mode vibration frequencies are scaled by correction factors⁷⁸ of 0.95 for CCSD and EOM-CCSD and 0.9614 for B3LYP.

As the hydrogen bonding topologies considered are quite varied, appropriate treatment of the basis-set superposition error (BSSE) is required in all atomic-basis set calculations. For small basis sets, the BSSE is large and the full counterpoise correction^{79,80} is essential to apply, whereas for large basis sets the correction is dramatically reduced and becomes smaller in magnitude than the extra binding that is facilitated by these larger basis sets so that its application enhances rather than reduces the associated errors.^{81,82} We use the fractional correction

$$E_{\text{fract}} = E_{\text{raw}} + \lambda E_{\text{BSSE}} \quad (2)$$

optimized⁴¹ for hydrogen-bonding interactions computed using medium-sized basis sets such as 6-31+G* and aug-cc-pVDZ, where E_{BSSE} is the usual counterpoise correction and $\lambda = 0.51$. One of the advantages of the use of plane-wave basis sets in the excited-state geometry optimizations performed using CPMD is the avoidance of the explicit BSSE corrections that are

required during the optimization of complexes of water interacting with electron-enhanced π -clouds of aromatic molecules.^{41,64}

3. Results and Discussion

Only a limited number of methods are available for excited-state geometry optimizations and frequency calculations, particularly when hydrogen bonds are involved. Before considering such calculations, it is essential to verify that realistic properties are predicted for the isolated pyrazine and water monomers as well as for the ground-state hydrogen bond. For reference, all ground and excited-state monomer and complex optimized geometries, vibration frequencies, and normal modes are provided in detail in Supporting Information.

3.1. Pyrazine and Water Monomers. In Table 1 are shown the root-mean-square (rms) errors between experimental^{83–86} structural parameters and vibrational frequencies of water and of pyrazine in their ground states (GS) and those calculated at the B3LYP and CCSD levels using both the cc-pVDZ and aug-cc-pVDZ basis sets. Full details of the calculated structures and normal modes are provided in Supporting Information, along with an enhanced summary in Table S1. In summary, all computed results are in good agreement with experiments. The test calculations performed using the aug-cc-pVDZ basis set show no significant improvement beyond the results obtained using cc-pVDZ.

Also shown in Table 1 are the results for the first (n,π*) and (π,π*) excited states calculated using the EOM-CCSD method. Only some of the vibrational frequencies have been experimentally determined^{83,84} for these two excited states (see Table S2 for full details), and the rms errors in the EOM-CCSD calculated frequencies are provided in Table 1. These errors of 46–82 cm⁻¹ are typically larger than those of 20–30 cm⁻¹ obtained for the ground state, perhaps because the most apparent modes in excited-state spectra are often those that are strongly vibronically active. As vibronically active modes have significantly different frequencies in the ground and excited states with the frequency shift being very sensitive to small errors in the perceived excited-state energy gaps, reduced accuracy is expected from ab initio prediction methods.

Shown in Table 2 are calculated and observed vertical and adiabatic excitation energies for the first (n,π*) and (π,π*) excited states of pyrazine. Although it is usual to approximate the observed vertical excitation energy as the frequency of the absorption maximum rather than the actual average excitation energy, in quantitative studies it is important to obtain the best possible experimental estimate, and values are available for pyrazine.^{71,72} The TD-B3LYP/cc-pVDZ gives accurate excitation energies for the (n,π*) state but overestimates the (π,π*) state energy by ca. 0.6 eV, whereas EOM-CCSD/cc-pVDZ more uniformly overestimates all transition energies by 0.3–0.5 eV.

TABLE 2: Calculated and Observed Vertical (E_v) and Adiabatic (E_0) Excitation Energies (in eV) for the First Singlet (n,π^*) States ${}^1B_{3u}$ and the First Singlet (π,π^*) States ${}^1B_{2u}$ of Pyrazine^a

method	E_v		E_0	
	(n,π^*)	(π,π^*)	(n,π^*)	(π,π^*)
EOM-CCSD/cc-pVDZ	4.45	5.19	4.33	4.96
EOM-CCSD/aug-cc-pVDZ	4.34	5.07	4.20	4.84
STEOM-CCSD/cc-pVDZ	4.18	4.77	4.07	4.51
TD-B3LYP/cc-pVDZ ^b	3.99	5.49	3.87	5.28
obs	3.98 ^c	4.81 ^d	3.83 ^e	4.69 ^e

^a At the geometry optimized at the EOM-CCSD level using cc-pVDZ or aug-cc-pVDZ basis sets. ^b From ref 71 and calculated the adiabatic excitation energies using D_{2h} optimized SCF ground state and CIS excited-state geometries. ^c Estimated as the observed 0–0 line at 3.83 eV⁸³ plus the reorganization energy of 0.15 eV from ref 71. ^d From ref 95. ^e From ref 83.

Much of the EOM-CCSD error is alleviated by increasing the basis set to aug-cc-pVDZ, however. Some test calculations are also performed using the more accurate but more demanding STEOM method, allowing the other major factor effecting the quality of the EOM-CCSD/cc-pVDZ results to be identified. From these results it is clear that EOM-CCSD/cc-pVDZ provides a very useful level of theory, being affordable with only systematic and qualitatively understood quantitative inadequacies.

The computed adiabatic energies should be adjusted for zero-point energy changes before comparisons can be made with experimental data, but it is not feasible to calculate this correction for each of the computational methods used. Our approach is therefore to determine “best estimated” zero-point energy changes using practicable computational methods. All computed zero-point energy changes are shown in Table 3, where our best-estimated values are defined; this approach has been applied more comprehensively^{41,64} for related systems than is demonstrated in the table, establishing that computed zero-point energies for excited-state hydrogen-bonded structures are somewhat insensitive to the computational method used. We actually apply this correction to the *observed* vertical excitation energies shown in Table 2 to obtain a quantity that may be directly compared with raw calculated values. Note, however, that both the zero-point energy corrections (–0.24 to +0.09 eV) and the difference between the vertical excitation energies and the band-maximum energies (ca. 0.15 eV) are large compared with the anticipated accuracy of modern computational methods; hence, in quantitative studies, their inclusion is essential.

3.2. H₂O:Pyrazine Complex. *3.2.1. Ground State.* This hydrogen-bonded complex has been the subject of many investigations,^{20,21,29,33–35,87–92} and its basic structure and energetics are known. As our interest is in vibrational analyses and excited states, we employ more approximate methods than have otherwise been used. Results are provided in Table 4 (key structural and energetic information), Figure 1 (structures), and Supporting Information (complete listing of structures, energies,

vibrational frequencies, and normal modes). Initially, we consider several possible structures for the H₂O:pyrazine complex analogous to those found for H₂O:pyridine,⁴¹ including two bifurcated structures with C_{2v} symmetry in which the water molecule is located either in-plane or perpendicular to the pyrazine, known as $C_{2v}(\text{planar})$ and $C_{2v}(\text{perp})$, respectively, and two analogous single hydrogen-bonded structures with C_s symmetry, known as $C_s(\text{planar})$ and $C_s(\text{perp})$. These four structures were optimized at the B3LYP and possibly CCSD levels using the cc-pVDZ and aug-cc-pVDZ basis sets; the optimized B3LYP/cc-pVDZ structures are shown in Figure 1 and the rather similar corresponding CCSD/cc-pVDZ structures are only provided in Supporting Information.

The calculated hydrogen-bond interaction energies ΔE , with and without fractional BSSE correction, are listed in Table 5. As B3LYP predicts that both the $C_s(\text{planar})$ and $C_s(\text{perp})$ structures are of much lower energy than their higher-symmetry variants, only these two structures are optimized using CCSD. Both methods predict very similar energies for $C_s(\text{planar})$ and $C_s(\text{perp})$, with $C_s(\text{planar})$, being more stable by 0.2 kcal mol^{–1}, taken as the reference configuration during subsequent excited-state studies. Clearly, structures of this generic linear hydrogen-bonded type can form over a wide range of the available configuration space. As shown in Figure 1, the $C_s(\text{planar})$ structure has the water molecule in plane with the pyrazine, and the $C_s(\text{perp})$ structure has the water in a perpendicular plane. Note that the $C_s(\text{planar})$ structure appears to gain stabilization from an additional interaction between the electron-deficient CH protons and the water oxygen.

The significance of BSSE is evident from Table 5 through the comparison of the relative energies of the various structures obtained using the cc-pVDZ and aug-cc-pVDZ basis sets with and without correction for BSSE, as well as through the plane-wave calculations. The plane-wave basis set used is very extensive and hence no BSSE calculations are required, but the use of a pseudopotential in these calculations constitutes an approximation of a different type. The $C_s(\text{planar})$ structure is calculated to be the lowest-energy one at the cc-pVDZ level by all methods, but this changes to $C_s(\text{perp})$ upon either expansion of the basis set or application of the BSSE correction. Also, the plane-wave results provide the same ordering pattern as do these enhanced calculations, with all absolute energies differing by at most 1 kcal mol^{–1}. It is hence clear that the accuracies achieved using the various basis sets and pseudopotentials is sufficient to allow the primary qualitative features of the hydrogen-bonding process to be adequately described.

Table 4 summarizes the geometric parameters and interaction energies calculated at the BLYP, B3LYP, and CCSD levels, together with previous theoretical results. Although CCSD predicts bond lengths intermediate between those of BLYP and B3LYP, all optimized structures are quite similar. Also, all methods predict that the hydrogen bonding induces only small changes in the geometrical parameters. For all the methods used, the predicted interaction energy falls in the range of –4.6 to –5.4 kcal mol^{–1}, with the “best estimates” being the B3LYP/

TABLE 3: Calculated Changes (in eV) in Zero-Point Energy upon Complex Formation or Excitation^a

	pyrazine+H ₂ O → H ₂ O:pyrazine			GS → (n,π^*)		GS → (π,π^*)	
	GS	(n,π^*)	(π,π^*)	pyrazine	H ₂ O:pyrazine	pyrazine	H ₂ O:pyrazine
(EOM-)CCSD/cc-pVDZ	0.072	0.088	–0.002	–0.237	–0.220	–0.042	–0.116
B3LYP/cc-pVDZ	0.074						
B3LYP/aug-cc-pVDZ	0.080						
best estimate	0.076	0.088	–0.002	–0.237	–0.220	–0.042	–0.116

^a Ignoring any intermolecular vibration of imaginary frequency.

TABLE 4: Calculated Interaction Energies ΔE (in kcal mol⁻¹) after Fractional BSSE Corrections and Key Geometric Parameters^a (Bond Length in Å and Bond Angles in Degrees) for the Electronic States of H₂O:Pyrazine

state	structure	geometry	$\Delta E/\text{kcal mol}^{-1}$												
			native	(EOM-)CCSD ^b	(TD-)B3LYP ^b	N ₁ H ₂	N ₄ H ₁₃	N ₁ O ₁₁	N ₄ O ₁₁	C ₂ N ₁ C ₆	C ₃ N ₄ C ₅	N ₁ H ₁₂ O ₁₁	N ₄ H ₁₃ O ₁₁	τ N ₁ C ₂ C ₃ N ₄	
GS	C _s (planar) ^c	BLYP/plane wave	-4.29	-4.62	2.139	2.981	116.1	115.7	0	0	0	0	0	0	0
		B3LYP/cc-pVDZ	-5.24	-4.62	2.039	2.867	115.7	141.3	0	0	0	0	0	0	0
		B3LYP/aug-cc-pVDZ	-5.22	-5.22	1.970	2.896	116.2	157.4	0	0	0	0	0	0	0
		CCSD/cc-pVDZ	-4.90	-4.45	2.102	2.931	115.6	142.4	0	0	0	0	0	0	0
(n,π*)	C _s (perp)	EOM-CCSD/cc-pVDZ	-4.74	-5.36	2.054	3.019	115.7	173.3	0	0	0	0	0	0	0
		EOM-CCSD/cc-pVDZ	-4.11	-4.36	2.110	2.941	121.7	142.7	0	0	0	0	0	0	0
		TD-BLYP/plane wave	-4.07	-2.98	2.116	2.979	117.7	142.3	0	0	0	0	0	0	0
		EOM-CCSD/cc-pVDZ	-4.07	-4.21	2.050	3.002	117.1	167.0	0	0	0	0	0	0	0
(π,π*)	C _s (perp)	C ₁ (top)		-0.37	2.493	3.346	4.328	134.0	1	1	134.0	1	1	1	1
		C ₁ (top)		-0.93	2.217	4.620	4.916	101.6	1	1	101.6	1	1	1	1
		C ₂ (bif)		0.42	3.208	3.887	3.887	126.7	10	10	126.7	10	10	10	10
		EOM-CCSD/cc-pVDZ	-5.42	-5.73	2.094	2.913	109.3	141.1	0	0	0	0	0	0	0
	C _s (perp)		-5.44	2.050	3.014	109.9	172.5	0	0	0	0	0	0	0	

^aThe atom numbers are defined in Figure 1. ^bCalculated using the aug-cc-pVDZ basis set. ^cOther values -5.4 kcal mol⁻¹ B3LYP/6-31+G**⁹², -4.3 kcal mol⁻¹ OPL- π -AA,³³ -7.3 kcal mol⁻¹ from AMBER molecular mechanics potential.²⁹ ^dOther value -4.3 kcal mol⁻¹ from AMBER molecular mechanics potential for the (n,π*)-decalocalized state.²⁹

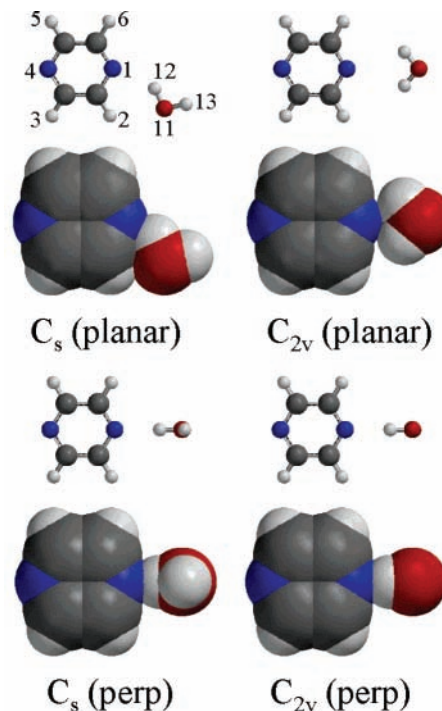


Figure 1. Hydrogen-bonded structures for the ground state of H₂O:pyrazine calculated at the B3LYP/cc-pVDZ level.

aug-cc-pVDZ value of -5.2 kcal mol⁻¹ and the CCSD/aug-cc-pVDZ value at the CCSD/cc-pVDZ geometry of -5.4 kcal mol⁻¹. These values are in good agreement with previous B3LYP/6-31+G** results⁹² (-5.4 kcal mol⁻¹) but are significantly less than estimates obtained using a specially developed AMBER molecular-mechanics potential²⁹ (-7.3 kcal mol⁻¹). Unfortunately, there is no available experimental hydrogen-bonding energy for comparison.

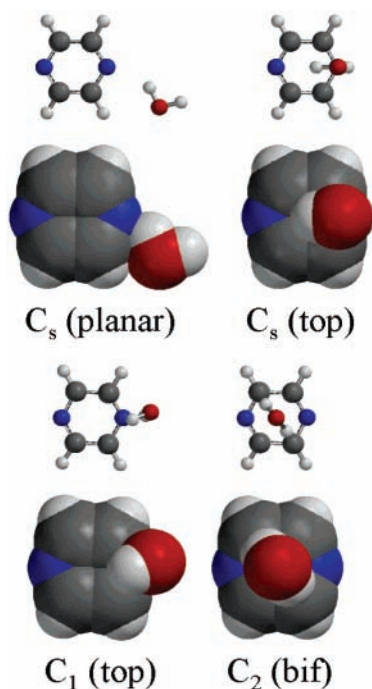
In Table S3, a detailed comparison is provided between observed and calculated vibrational frequencies for the complex. Only a small number of the vibration modes of pyrazine have been observed in aqueous solution⁹⁰ and/or for the H₂O:pyrazine complex.⁹⁰ The calculated vibration shifts are all in reasonable agreement with the available experimental values. A large red shift in the hydrogen-bonded OH stretch frequency is predicted, as expected on the basis of results for analogous systems,^{41,64} but no experimental data are available for comparison.

3.2.2. Lowest (n,π*) Excited State. Five different structures for the (n,π*) excited state of H₂O:pyrazine were optimized using TD-BLYP; the results are shown in Figure 2 (optimized structures), Table 4 (structural properties and fractional-BSSE-corrected interaction energies), and Supporting Information (optimized coordinates, normal-mode analyses, and analyses of frequency changes by mode). The lowest-energy structure, named C_s(planar), is analogous to the lowest-energy structure found for the ground state; it has also been optimized using EOM-CCSD/cc-pVDZ. Also similar to the ground-state hydrogen bonding, the C_s(perp) structure is found at slightly higher energy than is C_s(planar). Of the other structures, one named C₂(bif) has the water above the π-plane with both hydrogens interacting symmetrically with the π-cloud of pyrazine. This structure was optimized without use of symmetry and the symmetric structure resulted. The other two structures again have the water above the plane, but in each case one hydrogen interacts directly with a nitrogen atom from above; the other hydrogen points either toward the π cloud (named C_s(top)) or away from it (named C₁(top)).

TABLE 5: Calculated Interaction Energies ΔE (in kcal mol⁻¹), for Water to the Ground State of Pyrazine at Different Possible Structures (See Figure 1), with and without Fractional BSSE Correction

structure	B3LYP				BLYP				CCSD				
	cc-pVDZ		aug-cc-pVDZ		plane-wave E_{raw}	cc-pVDZ ^a		aug-cc-pVDZ ^a		cc-pVDZ		aug-cc-pVDZ ^b	
	E_{raw}	E_{fract}	E_{raw}	E_{fract}		E_{raw}	E_{fract}	E_{raw}	E_{fract}	E_{raw}	E_{fract}	E_{raw}	E_{fract}
C_{2v} (planar)	-3.55	-2.36	-1.43	-1.27	-3.11	-3.28	-2.73	-2.18	-2.08				
C_{2v} (perp)	-4.82	-3.21	-2.15	-2.02	-2.01	-3.63	-2.45	-1.41	-1.30				
C_s (planar)	-6.85	-5.24	-5.52	-5.22	-3.68	-5.79	-4.29	-3.78	-3.48	-6.44	-5.97	-6.04	-5.38
C_s (perp)	-6.71	-5.28	-5.48	-5.28	-4.72	-5.57	-4.25	-4.16	-3.97	-6.07	-4.74	-5.75	-5.18

^a At the BLYP/plane-wave optimized structure. ^b At the CCSD/cc-pVDZ optimized structure.

**Figure 2.** Hydrogen-bonded structures for the (n,π^*) excited state of $\text{H}_2\text{O}:\text{pyrazine}$ calculated at the TD-BLYP/plane-wave level.

As indicated by the optimized values for torsional angles $\text{N}_1\text{C}_2\text{N}_3\text{C}_4$ given in Table 4 (see Figure 1 for the atomic numbering), the pyrazyl plane remains nearly planar for all structures except the doubly π -cloud bonded structure $C_2(\text{bif})$, for which it is only 10° . This result is in stark contrast to that found for analogous structures of $\text{H}_2\text{O}:\text{pyridine}$;⁴¹ for it, the excited-state equilibrium hydrogen-bonded structure undergoes a large boat distortion with torsional angles $>30^\circ$, this distortion arising primarily from modulation of the strong vibronic coupling between the ${}^1\text{B}_1(n,\pi^*)$ state of interest and a nearby ${}^1\text{A}_1(\pi,\pi^*)$ state. It is hence clear that the excited-state hydrogen bonding in $\text{H}_2\text{O}:\text{pyrazine}$ is fundamentally different from that in $\text{H}_2\text{O}:\text{pyridine}$, being more similar to that found for $\text{H}_2\text{O}:\text{pyrimidine}$.⁶⁴

The fractional-BSSE-corrected interaction energy ΔE from Table 4 evaluated using EOM-CCSD for the lowest-energy C_s -(planar) structure is -4.4 kcal mol⁻¹, only 1.0 kcal mol⁻¹ less bound than the corresponding ground-state structure. This result is also similar to that found for $\text{H}_2\text{O}:\text{pyrimidine}$ ⁶⁴ but in stark contrast to that found for $\text{H}_2\text{O}:\text{pyridine}$ ⁴¹ as, for the latter, the ground-state structure is destabilized on the excited-state sufficient that it no longer remains a local-minimum configuration, relaxing without barrier to either dissociate or reach alternate above-ring π -cloud bonded structures. These alternate structures for $\text{H}_2\text{O}:\text{pyrazine}$ have only been optimized using TD-BLYP but consistently appear to be 1.5 – 4 kcal mol⁻¹ higher in energy than $C_s(\text{planar})$. The most strongly bound structure is $C_1(\text{top})$

as this facilitates the best interaction with a nitrogen, and the doubly bonded structure to the π -cloud, $C_2(\text{bif})$, is the least stable structure.

The differences in the hydrogen-bonding found in $\text{H}_2\text{O}:\text{pyrazine}$, $\text{H}_2\text{O}:\text{pyrimidine}$ ⁶⁴ and $\text{H}_2\text{O}:\text{pyridine}$ ⁴¹ can be understood in terms of the degree of involvement in the transition of the nitrogen lone pair that is not hydrogen bonded. The calculated C–N–C bond angles for $\text{H}_2\text{O}:\text{pyrazine}$ at the EOM-CCSD are 118° (hydrogen-bonded nitrogen) and 122° (free nitrogen), and those for $\text{H}_2\text{O}:\text{pyrimidine}$ are 118° and 130° , respectively, and that for $\text{H}_2\text{O}:\text{pyridine}$ is 129° . These values indicate that the (n,π^*) excitation is strongly localized on just one of the two nitrogens in $\text{H}_2\text{O}:\text{pyrimidine}$ but remains closer to the fully delocalized (equal angle) limit than to the fully localized (ca. $118^\circ/130^\circ$) case. Note that, for both pyrimidine⁶⁴ and pyrazine,²⁹ the (n,π^*) excitation is fully delocalized over both nitrogens in isolated molecules, the CNC angles being 121° in pyrazine (Table S1) and 123° in pyrimidine.⁶⁴ Hence hydrogen bonding to pyrimidine is predicted to affect the electronic structure of the chromophore in a much more profound way than it bonding to pyrazine. The AMBER molecular-mechanics force field for pyrazine in its hypothetical fully delocalized (n,π^*) state predicts a binding energy with water²⁹ of 4.7 kcal mol⁻¹, close to the B3LYP and CCSD values of 5.2 – 5.4 kcal mol⁻¹ (Table 4). Despite the loss of lone-pair electron density, both this approach and the CCSD and B3LYP methods predict that the excited-state hydrogen bond is more stable in $\text{H}_2\text{O}:\text{pyrazine}$ ²⁹ compared to $\text{H}_2\text{O}:\text{pyrimidine}$ ^{26,41} by 0.6 kcal mol⁻¹.

In Table 6 is shown a variety of deduced energetic parameters for the (n,π^*) excited states of $\text{H}_2\text{O}:\text{pyrazine}$, obtained for the investigation of excited-state dynamical properties. The quantities involved are sketched in Figure 3 and include the appropriate zero-point energies E_{zpt} , interaction energies ΔE , complex vertical (E_v), adiabatic (E_0), and origin (E_{00}) transition energies, as well as the adiabatic transition energy in isolated pyrazine, $E_0(\text{Pz})$. This figure is sketched along an idealized coordinate that starts from the linear hydrogen-bonded structure of the ground state on to molecular dissociation. The excited-state minimum is indeed accessible without barrier from the ground-state geometry, as indicated qualitatively in the figure. In addition, two other energies provide indicators of the types of dynamics likely on the excited-state potential-energy surface. First there is the predissociation energy

$$E_{\text{pre}} = E_{00}(\text{Pz}) - \Delta E^{\text{GS}} - \Delta E_{\text{zpt}}^{\text{GS}} \quad (3)$$

which specifies the minimum energy for optical excitation that could possibly lead to dissociation of the complex in the excited state, where $E_{00}(\text{Pz})$ is the 0–0 transition energy of gas-phase pyrazine and $\Delta E_{\text{zpt}}^{\text{GS}}$ is the change in zero-point energy due to complex formation in its ground electronic state. For dissociation to occur at this excitation energy, all energy imparted into

TABLE 6: Calculated Vertical Excitation Energies (E_v) as Well as Fractional BSSE-Corrected Original Energies (E_{00}), Predissociation Energies (E_{pre}) for H₂O:Pyrazine in Its (n,π^*) and (π,π^*) Excited States, after Correction for Errors in the Calculations of Isolated Pyrazine (All in eV)^a

method	H ₂ O:pyrazine (n,π^*)						H ₂ O:pyrazine (π,π^*)					
	$E_v - E_v(\text{Pz})$	E_v	E_{dir}	E_{pre}	E_{00}	$E_{00} - E_{00}(\text{Pz})$	$E_v - E_v(\text{Pz})$	E_v	E_{dir}	E_{pre}	E_{00}	$E_{00} - E_{00}(\text{Pz})$
EOM-CCSD/cc-pVDZ	0.06	4.04	4.06	3.91	3.88	0.05	-0.02	4.79	4.89	4.77	4.60	-0.09
EOM-CCSD/aug-cc-pVDZ	0.06	4.04	4.11	3.96	3.89	0.06	-0.02	4.79	4.94	4.82	4.60	-0.09
exp					3.87 ^b	0.04 ^b						
					3.90 ^c	0.07 ^c						
pyrazine monomer		3.98 ^d			3.83 ^e			4.81 ^f			4.69 ^e	

^a At the EOM-CCSD/cc-pVDZ optimized geometry. ^b From ref 87 in solid neon. ^c From ref 8 in molecular beam. ^d Estimated as the observed 0–0 line at 3.83 eV⁸³ plus the reorganization energy of 0.15 eV. from ref 72. ^e From ref 83. ^f From ref 95.

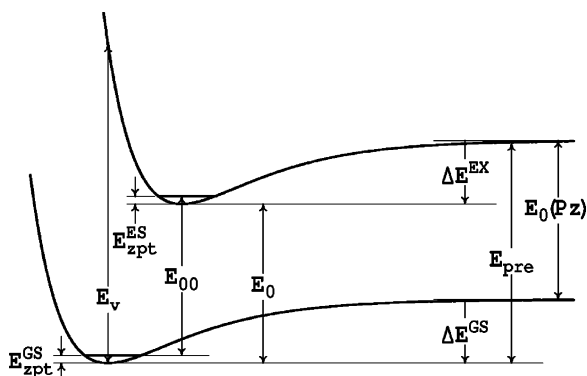


Figure 3. Schematic potential-energy surfaces for the ground state (GS) and an excited state (ES) of H₂O:pyrazine as a function of some dissociative intermolecular coordinate, indicating the adiabatic excitation energy of pyrazine monomer, $E_0(\text{Pz})$, the vertical, adiabatic, and origin transition energies of the complex, E_v , E_0 , and E_{00} , respectively, the zero-point energies $E_{\text{zpt}}^{\text{GS}}$ and $E_{\text{zpt}}^{\text{ES}}$, and the hydrogen-bond interaction energies ΔE^{GS} and ΔE^{ES} .

vibrational motions of the pyrazine molecule must be converted into translational energy of the fragments, however. This energy is also indicated in Figure 3; the second energy is that required for direct dissociation *without* the need for energy transfer from the excited vibrations of pyrazine. As this energy is dependent on the specific vibronic level of the complex being excited, we consider only excitation at the band center and express the band-center direct dissociation energy as

$$E_{\text{dir}} = E_v(\text{Pz}) - \Delta E^{\text{GS}} - \Delta E_{\text{zpt}}^{\text{GS}} \quad (4)$$

where $E_v(\text{Pz})$ is the vertical excitation energy of the gas-phase pyrazine.

Table 6 provides best estimated predictions of the actual molecular properties by correcting the computed transition energies for the known errors of each particular method in predicting the transition energies of isolated pyrazine. In this fashion, E_v and E_{00} for the complex are evaluated by adding to the calculated value of $E_v - E_v(\text{Pz})$ and the observed value for $E_v(\text{Pz})$, etc.

For the (n,π^*) excited state, the EOM-CCSD calculations predict that the predissociation energy E_{pre} of the complex is in excess of the 0–0 energy E_{00} by only ca. 0.03–0.07 eV, hence suggesting that a bound excited-state complex is possible. Further, the vertical excitation energy E_v is predicted to exceed the dissociation energy by only ca. 0.1 eV, indicating that irradiating the gas-phase complex in its ground state should produce a measurable level of the bound excited-state complex. However, the vertical excitation energy is predicted to be close to the direct dissociation energy E_{dir} so that energy transfer from intramolecular modes to intermolecular motions is not required for the major fraction of the vertically excited complex to

predissociate so that the dissociation process is expected to be very rapid. Similar calculations for H₂O:pyridine⁴¹ predict the vertically excited state is purely dissociative in nature and those for H₂O:pyrimidine⁶⁴ predict significantly enhanced excited-state stability. The reduced stability for H₂O:pyrazine is consistent with the enhanced degree of (n,π^*) delocalization implied by the similar values, 118° and 122°, calculated for the two CNC bond angles. Even a fully delocalized excited state is not expected to lead to a broken excited-state hydrogen bond as in this limit 1.5 electrons still remain in the hydrogen-bonded lone-pair orbital after excitation.²⁹

The calculated hydrogen-bonding shift to the origin energy $E_{00} - E_{00}(\text{Pz})$ is 0.05–0.06 eV (see Table 6), in good agreement with the experimentally observed range of 0.04–0.07 eV.^{8,87} Such shifts are much less than those calculated by similar methods for H₂O:pyrimidine, 0.10–0.12 eV,⁶⁴ as well as for H₂O:pyridine, 0.16–0.21 eV.⁴¹ The large value for H₂O:pyridine is due to the weakness of the excited-state interaction, and the midrange value for H₂O:pyrimidine arises not because the excited-state bond is weaker than that for H₂O:pyrazine, but rather because the ground-state hydrogen bond is stronger. Simulated using AMBER molecular-mechanics potential-energy surfaces for the ground and fully delocalized excited states,²⁹ the shift for H₂O:pyrazine is calculated to be 0.12 eV and is overestimated due to the overbinding predicted by this method of water to the ground state of pyrazine.

As shown in Figure 3, the blue shift of the (n,π^*) band is indicative of the energy required to break the ground-state hydrogen bond. In aqueous solution, the observed blue shift of the pyrazine (n,π^*) band is 0.20–0.25 eV,^{4,83} much larger than the values calculated and observed for the H₂O:pyrazine complex. Both ab initio simulations using dielectric-continuum models to represent the liquid^{38,39,42} and fully polarized solvent-shift calculations using explicit solvent structures^{29,93} indicate that the structure of the liquid is important in determining the observed solvent shift, with long-range interactions contributing significantly. However, the blue shift for the linear H₂O:pyrazine:H₂O complex is expected⁶⁴ to be more indicative of the value in solution than is that for the monomeric complex studied herein.

3.2.3. Lowest (π,π^*) Excited State. The TD-BLYP and EOM-CCSD calculations predict that H₂O:pyrazine in its first (π,π^*) excited state has a C_s (planar) structure similar to those optimized for the ground and first (n,π^*) excited states, with a corresponding C_s (perp) structure slightly higher in energy. The calculated bonding energy and geometric parameters are shown in Table 4. Although for C_s (planar) the intermolecular hydrogen-bonding parameters $R(\text{N}_1-\text{H}_{12})$, $R(\text{N}_1-\text{O}_{11})$ and $\angle \text{N}_1-\text{H}_{12}-\text{O}_{11}$ are very similar for the (n,π^*) and (π,π^*) interactions, the pyrazine C–N–C angle (116° in the ground state and 118°/122° in the (n,π^*) state) contracts to 109°, indicating the nitrogens have adopted sp³ hybridization, suggesting the pres-

ence of two lone pairs. Indeed, the EOM-CCSD calculated hydrogen-bond strength increases by 0.4 kcal mol⁻¹ compared to the CCSD ground-state strength, in contrast to the (n,π*) state for which the bond strength decreased by 1.0 kcal mol⁻¹.

The calculated negative values of $E_v - E_v(\text{Pz})$ and $E_{00} - E_{00}(\text{Pz})$ (see Table 6) predict that the (π,π*) absorption of H₂O:pyrazine should display a small red shift (~160 cm⁻¹), in contrast to the blue shift (~500 cm⁻¹) predicted for the (n,π*) absorption. Such shifts are typical of (π,π*) absorptions of pyrazine and other azines in dilute solution⁴ and are consistent with other calculations.⁴²

Overall, quite a different *scenario* is predicted for the first (π,π*) excited state compared to the (n,π*) state. Only small changes in the vertical and adiabatic transition energies are predicted upon complex formation, as are observed. The vertical excitation energy E_v is calculated to be either less than or close to the predissociation energy E_{pre} and the direct dissociation energy E_{dir} , suggesting that the complex may be long-lived. However, energy relaxation from the (π,π*) state to the (n,π*) state will be rapid, leading to dissociation of the complex.

4. Conclusions

The lowest-energy hydrogen-bonded structures for the H₂O:pyrazine complex in its ground state, first (n,π*) excited state, and first (π,π*) excited state are all predicted to be planar with the water offering a linear hydrogen bond to a pyrazine nitrogen, there being also a weak interaction between the pyrazine ortho hydrogen and the water oxygen. All hydrogen bonds are predicted to be quite strong, ca. 5.4 kcal mol⁻¹ for the ground state, 4.4 kcal mol⁻¹ for the (n,π*) excited state, and 5.7 kcal mol⁻¹ for the (π,π*) state, after zero-point energy and BSSE correction.

Although the intermolecular hydrogen-bonding geometries are similar for the hydrogen bonds to the three states of pyrazine, significant differences are predicted for the intramolecular pyrazine CNC angles. In the (π,π*) excited state these angles contract uniformly toward sp³ hybridization but they expand and differentiate in the (n,π*) state. This differentiation is indicative of the tendency for the excitation to localize on the non-hydrogen-bonded nitrogen, but the effect is small, just 4° compared to the value of 13° predicted by similar calculations for the H₂O:pyrimidine complex⁶⁴ for which the localization is nearly complete. A molecular-mechanics potential²⁹ for water interacting with the (n,π*) excited state, assumed to have a completely delocalized excitation, is shown to provide a realistic description of the interaction, in contrast⁶⁴ to a similar potential²⁷ for H₂O:pyrimidine. Despite the loss of lone-pair electron density due to this delocalization, the (n,π*) hydrogen bond is calculated to be 0.6 kcal mol⁻¹ stronger for H₂O:pyrazine than for H₂O:pyrimidine,⁶⁴ and this, combined with an enhanced predicted stability for the ground-state hydrogen bond in the complex with pyrimidine, explains the observed small value of the blue shift for H₂O:pyrazine.⁸ These calculations, along with results indicating significant long-range contributions^{29,38,39,42} to the observed⁴ much larger blue shift in dilute solution, provide a framework in which the aqueous solvation of pyrazine can be interpreted.

Although the vertically excited (π,π*) state is predicted to be stable with respect to direct dissociation, it should quickly convert to the lower energy (n,π*) state. For this state, the calculated predissociation energy E_{pre} is in excess of the 0–0 energy by only 0.03–0.07 eV, however, and so the excited states are predicted to be only short-lived. These calculations thus can explain the failure to detect diazine–water complexes after

excitation to excited states⁸ in two-color time-of-flight mass spectroscopic studies.⁸ However, alternate explanations are also possible such as internal conversion⁹⁴ of the (n,π*) state to the ground state during the time-of-flight of the complex.⁸

Previously, two motifs have been identified for the hydrogen bonding of water with the excited states of azines. For H₂O:pyridine, the hydrogen bond is broken by the removal of one of the lone-pair electrons from the nitrogen, leading to spontaneous dissociation of the vertically excited complex.⁴¹ Nevertheless, strong hydrogen bonds are predicted to form between water and the electron-rich π-cloud of pyridine. For H₂O:pyrimidine, localization of the (n,π*) excitation on the non-hydrogen-bonded nitrogen leads instead to a strong excited-state hydrogen bond that is predicted to be reasonably stable after vertical excitation.⁶⁴ Here, for H₂O:pyrazine, we find that the (n,π*) excitation remains quite delocalized, leading to only tenuous stability of excited-state complexes. Excited-state hydrogen-bonding thus shows a richness arising from the coupling of the motion of the excited electron with the intramolecular nuclear vibrations.

Acknowledgment. We thank the Australian Research Council for funding this research and the Australian Partnership for Advanced Computing for the provision of computational resources.

Supporting Information Available: Provided are the Tables S1–S4 in pdf format describing the calculated and observed^{83,84,90,96,97} frequency changes on formation of H₂O:pyrazine in its ground and excited states, along with the calculated intermolecular vibration frequencies, along with the complete version of refs 73–75. All optimized structures, vibration frequencies, and normal modes for the complex and its structures, as well as pertinent Duschinsky rotation matrices and geometry changes projected onto normal coordinates are also provided in ASCII txt format. This material is available free via the Internet at <http://pubs.acs.org>.

References and Notes

- Rablen, P. R.; Lockman, J. W.; Jorgensen, W. L. *J. Phys. Chem. A* **1998**, *102*, 3782.
- Jeffrey, G. A.; Saenger, W. *Hydrogen bonding in biological structure*; Springer-Verlag: Berlin, 1991.
- Beratan, D. N.; Hopfield, J. J. *Am. Chem. Soc.* **1984**, *106*, 1584.
- Baba, H.; Goodman, L.; Valenti, P. C. *J. Am. Chem. Soc.* **1966**, *88*, 5410.
- Mctigue, P.; Renowden, P. V. *J. Chem. Soc., Faraday I* **1975**, 1784.
- Carrabba, M. M.; Kenny, J. E.; Moomaw, W. R.; Cordes, J.; Denton, M. *J. Phys. Chem.* **1985**, *89*, 674.
- Schauer, M.; Bernstein, E. R. *J. Chem. Phys.* **1985**, *82*, 726.
- Wanna, J.; Menapace, J. A.; Bernstein, E. R. *J. Chem. Phys.* **1986**, *85*, 1795.
- Wanna, J.; Bernstein, E. R. *J. Chem. Phys.* **1987**, *86*, 6707.
- Maes, G.; Smets, J. *J. Mol. Struct.* **1992**, *270*, 141.
- Destexhe, A.; Smets, J.; Adamowicz, L.; Maes, G. *J. Phys. Chem.* **1994**, *98*, 1506.
- Zoidis, E.; Yarwood, J.; Danten, Y.; Besnard, M. *Mol. Phys.* **1995**, *85*, 373.
- Zoidis, E.; Yarwood, J.; Danten, Y.; Besnard, M. *Mol. Phys.* **1995**, *85*, 385.
- Buyl, F.; Smets, J.; Maes, G.; Adamowicz, L. *J. Phys. Chem.* **1995**, *99*, 14967.
- Del Bene, J. E.; Person, W.; Szczepaniak, K. *Mol. Phys.* **1996**, *89*, 47.
- Szczepaniak, K.; Chabrier, P.; Person, W. B.; Del Bene, J. E. *J. Mol. Struct.* **1997**, *436–437*, 367.
- Mccarthy, W.; Smets, J.; Adamowicz, L.; Plokhotzichenos, A. M.; Radchenko, E. D.; Shenja, G. G.; Stepanian, S. G. *Mol. Phys.* **1997**, *91*, 513.
- Melandri, S.; Sanz, M. E.; Caminati, W.; Favero, P. G.; Kisiel, Z. *J. Am. Chem. Soc.* **1998**, *120*, 11504.
- Zhang, B.; Cai, Y.; Mu, X.; Lou, N.; Wang, X. *J. Chem. Phys.* **2002**, *117*, 3701.

- (20) Del Bene, J. E. *J. Am. Chem. Soc.* **1975**, *97*, 5330.
(21) Del Bene, J. E. *Chem. Phys.* **1976**, *15*, 463.
(22) Del Bene, J. E. *Chem. Phys.* **1980**, *50*, 1.
(23) Del Bene, J. E. *J. Comput. Chem.* **1981**, *2*, 422.
(24) Zeng, J.; Craw, J. S.; Hush, N. S.; Reimers, J. R. *J. Chem. Phys.* **1993**, *99*, 1482.
(25) Zeng, J.; Craw, J. S.; Hush, N. S.; Reimers, J. R. *Chem. Phys. Lett.* **1993**, *206*, 323.
(26) Zeng, J.; Hush, N. S.; Reimers, J. R. *J. Chem. Phys.* **1993**, *99*, 1496.
(27) Zeng, J.; Hush, N. S.; Reimers, J. R. *J. Chem. Phys.* **1993**, *99*, 1508.
(28) Del Bene, J. E. *J. Phys. Chem.* **1994**, *98*, 5902.
(29) Zeng, J.; Woywod, C.; Hush, N. S.; Reimers, J. R. *J. Am. Chem. Soc.* **1995**, *117*, 8618.
(30) Zeng, J.; Hush, N. S.; Reimers, J. R. *J. Phys. Chem.* **1996**, *100*, 9561.
(31) Maes, G.; Smets, J.; Adamowicz, L.; McCarthy, W.; Van Bael, M. K.; Houben, L.; Shoone, K. *J. Mol. Struct.* **1997**, *410–411*, 315.
(32) Gao, J.; Byun, K. *Theor. Chim. Acta* **1997**, *96*, 151.
(33) Jorgensen, W. L.; McDonald, N. A. *J. Mol. Struct. (THEOCHEM)* **1998**, *424*, 145.
(34) Caminati, W.; Moreschini, P.; Favero, P. G. *J. Phys. Chem. A* **1998**, *102*, 8097.
(35) Caminati, W.; Favero, L. B.; Favero, P. G.; Maris, A.; Melandri, S. *Angew. Chem., Int. Ed.* **1998**, *37*, 792.
(36) de Almeida, K. J.; Coutinho, K.; de Almeida, W. B.; Rocha, W. R.; Canuto, S. *Phys. Chem. Chem. Phys.* **2001**, *3*, 1583.
(37) Martin, M. E.; Sanchez, M. L.; Aguilar, M. A.; del Valle, F. J. O. *J. Mol. Struct. (THEOCHEM)* **2001**, *537*, 213.
(38) Cossi, M.; Barone, V. *J. Chem. Phys.* **2001**, *115*, 4708.
(39) Mennucci, B. *J. Am. Chem. Soc.* **2002**, *124*, 1506.
(40) Ramaekers, R.; Houben, L.; Adamowicz, L.; Maes, G. *Vibr. Spectrosc.* **2003**, *32*, 185.
(41) Cai, Z. -L.; Reimers, J. R. *J. Phys. Chem. A* **2002**, *106*, 8769.
(42) de Monte, S. A.; Mueller, T.; Dallos, M.; Lischka, H.; Diedenhofen, M. *Theor. Chem. Acc.* **2004**, *111*, 78.
(43) Del Bene, J. E.; Gwaltney, S. R.; Bartlett, R. J. *J. Phys. Chem. A* **1998**, *102*, 5124.
(44) Chaban, G. M.; Gordon, M. S. *J. Phys. Chem. A* **1999**, *103*, 185.
(45) Organero, J. A.; Douhal, A.; Santos, L.; Martinez-Ataz, E.; Guallar, V.; Moreno, M.; Lluch, J. M. *J. Phys. Chem. A* **1999**, *103*, 5301.
(46) McRae, E. G. *J. Phys. Chem.* **1957**, *61*, 562.
(47) Liptay, W. In *Modern quantum chemistry*; Sinanoglu, O., Ed.; Academic Press: New York, 1965; Vol. III, p 45.
(48) Rettig, W. *J. Mol. Struct.* **1982**, *84*, 303.
(49) Kleier, D. A.; Martin, R. L.; Wadt, W. R.; Moomaw, W. R. *J. Am. Chem. Soc.* **1982**, *104*, 60.
(50) Karelson, M. M.; Zerner, M. C. *J. Am. Chem. Soc.* **1990**, *112*, 9405.
(51) Karelson, M. M.; Zerner, M. C. *J. Phys. Chem.* **1992**, *96*, 6949.
(52) Hush, N. S.; Reimers, J. R. *Coord. Chem. Rev.* **1998**, *177*, 37.
(53) Malaspina, T.; Coutinho, K.; Canuto, S. *J. Chem. Phys.* **2002**, *117*, 1692.
(54) Weiner, S. J.; Kollman, P. A.; Nguyen, D. T.; Case, D. A. *J. Comput. Chem.* **1986**, *7*, 230.
(55) CPMD (*Car-Parrinello Molecular Dynamics*); IBM Corp. and MPI fuer Festkoerprforschung: Stuttgart, 1997–2001.
(56) Jorgensen, W. L.; McDonald, N. A. *J. Mol. Struct. (THEOCHEM)* **1998**, *424*, 145.
(57) Spoliti, M.; Bencivenni, L.; Ramondo, F. *THEOCHEM* **1994**, *303*, 185.
(58) Smets, J.; Adamowicz, L.; Maes, G. *J. Mol. Struct.* **1994**, *322*, 113.
(59) Martoprawiro, M. A.; Bacskay, G. B. *Mol. Phys.* **1995**, *85*, 573.
(60) Samanta, U.; Chakrabarti, P.; Chandrasekhar, J. *J. Phys. Chem. A* **1998**, *102*, 8964.
(61) Smets, J.; McCarthy, W.; Maes, G.; Adamowicz, L. *J. Mol. Struct.* **1999**, *476*, 27.
(62) Dkhissi, A.; Adamowicz, L.; Maes, G. *J. Phys. Chem.* **2000**, *104*, 2112.
(63) Papai, I.; Jancso, G. *J. Phys. Chem.* **2000**, *104*, 2132.
(64) Cai, Z. -L.; Reimers, J. R. *J. Phys. Chem. A* **2005**, *109*, 1576.
(65) Becke, A. D. *J. Chem. Phys.* **1993**, *98*, 5648.
(66) Becke, A. D. *Phys. Rev. A* **1988**, *38*, 3098.
(67) Lee, C.; Yang, W.; Parr, R. G. *Phys. Rev. B* **1988**, *37*, 785.
(68) Purvis, G. D., III; Bartlett, R. J. *J. Chem. Phys.* **1982**, *76*, 1910.
(69) Stanton, J. F.; Bartlett, R. J. *J. Chem. Phys.* **1993**, *98*, 7029.
(70) Nooijen, M.; Bartlett, R. J. *J. Chem. Phys.* **1997**, *106*, 6441.
(71) Weber, P.; Reimers, J. R. *J. Phys. Chem. A* **1999**, *103*, 9821.
(72) Weber, P.; Reimers, J. R. *J. Phys. Chem. A* **1999**, *103*, 9830.
(73) Frisch, M. J.; Trucks, G. W.; Schlegel, H. B.; et al. *GAUSSIAN 98 Rev. A7*; Gaussian Inc.: Pittsburgh, 1998.
(74) Ahlrichs, R.; Bär, M.; Baron, H. -P.; et al. *TURBOMOLE*, Version 5.2; Quantum Chemistry Group, The University of Karlsruhe: Karlsruhe, 2002.
(75) Stanton, J. F.; Gauss, J.; Watts, J. D.; et al. *ACES II*; Quantum Theory Project, The University of Florida: Gainesville, 1999.
(76) Dunning, T. H., Jr. *J. Chem. Phys.* **1989**, *90*, 1007.
(77) Kendall, R. A.; Dunning, T. H., Jr.; Harrison, R. J. *J. Chem. Phys.* **1992**, *96*, 6796.
(78) Scott, A. P.; Radom, L. *J. Phys. Chem.* **1996**, *100*, 16502.
(79) Boys, S. F.; Bernardi, F. *Mol. Phys.* **1970**, *19*, 553.
(80) van Duijneveldt, F. B.; van Duijneveldt-van de Rijdt, G. C.; van Leuven, J. H. *Chem. Rev.* **1994**, *94*, 1973.
(81) Dunning, T. H., Jr. *J. Phys. Chem. A* **2000**, *104*, 9062.
(82) Lambropoulos, N. A.; Reimers, J. R.; Hush, N. S. *J. Chem. Phys.* **2002**, *116*, 10277.
(83) Innes, K. K.; Ross, I. G.; Moomaw, W. R. *J. Mol. Spectrosc.* **1988**, *132*, 492.
(84) Suzuka, I.; Udagawa, Y.; Ito, M. *Chem. Phys. Lett.* **1979**, *64*, 333.
(85) Hoy, A. R.; Bunker, P. B. *J. Mol. Spectrosc.* **1974**, *74*, 1.
(86) Herzberg, G. *Molecular spectra and molecular structure. III. Electronic spectra and electronic structure of polyatomic molecules*; D. Van Nostrand: Princeton, 1966.
(87) Rossetti, R.; Brus, L. E. *J. Chem. Phys.* **1979**, *70*, 4730.
(88) Brolo, A. G.; Irish, D. E. *Naturforsch* **1995**, *50a*, 274.
(89) Nobeli, I.; Price, S. L.; Lommerse, J. P. M.; Taylor, R. *J. Comput. Chem.* **1997**, *18*, 2060.
(90) Montanez, M. A.; Tocon, I. L.; Otero, J. C.; Marcos, J. I. *J. Mol. Struct.* **1999**, *482–483*, 201.
(91) Hush, N. S.; Reimers, J. R. *Chem. Rev.* **2000**, *100*, 775.
(92) Kim, J. H.; Lee, H.-J.; Kim, E.-J.; Jung, H. J.; Choi, Y.-S.; Park, J.; Yoon, C.-J. *J. Phys. Chem. A* **2004**, *108*, 921.
(93) Zeng, J.; Hush, N. S.; Reimers, J. R. *Chem. Phys. Letters* **1993**, *206*, 318.
(94) Sobolewski, A. L.; Woywod, C.; Domcke, W. *J. Chem. Phys.* **1993**, *98*, 5627.
(95) Walker, I. C.; Palmer, M. H. *Chem. Phys.* **1991**, *153*, 169.
(96) Craddock, S.; Liescheski, P. B.; Rankin, D. W. H.; Robertson, H. E. *J. Am. Chem. Soc.* **1988**, *110*, 2758.
(97) Innes, K. K.; Byrne, J. P.; Ross, I. G. *J. Mol. Spectrosc.* **1967**, *22*, 125.